Torque Pattern Generation Towards the Maximum Jump Height

Mitsuru Higashimori, Manabu Harada, Idaku Ishii and Makoto Kaneko
Department of Artificial Complex Systems Engineering
Graduate School of Engineering, Hiroshima University
Kagamiyama 1-4-1, Higashi-Hiroshima 739-8527, Japan
Email: higashi@hfl.hiroshima-u.ac.jp

***Abstract*— This paper discusses jumping pattern generation for a serial link robot in order to maximize its jump height under torque limitation. By applying a genetic algorithm (GA) for determining torque assignment, we obtain various jumping patterns with respect to the torque limitation for a fixed mass of the robot. With the increase of the torque limitation, double-leg based jump, single-leg based jump, and spring-type jump are generated for achieving the largest jump height. Under an additional joint angle limitation, we also obtain an interesting solution where one end of the link is first lifted up and the other end finally kicks the ground strongly.**

I. INTRODUCTION

Legged robots can be classified into two groups; static based locomotion where the center of gravity is always kept within the support polygon constructed by the supporting legs, and dynamic based locomotion where the center of gravity is allowed to exit the support polygon. The latter category also contains jumping robots [1]–[7] which can be expected to be able to move through environments containing bumps. While various jumping robots have been proposed so far, accumulated energy using either spring or pneumatic actuator is utilized for most of them. Such actuation mechanisms are specially designed for the jumping motion and a dexterity of legs is not considered as the primary target. On the other hand, a higher dexterity of legs can be expected by utilizing a rotational type motor for controlling each leg in a jumping robot. This motor should be extremely light and powerful motor. With the recent increase of actuation technique, however it has become possible to realize a jumping robot driven by a rotational type motor. Hayashi et al. [5] have developed a pendulum-type jumping machine utilizing the swing motion of the arm where the joint motion is generated by a rotational type motor. Arikawa et al. [6] have developed the multi-DOF jumping robot. They have discussed planning parameters of robot motions for achieving jumping and somersault. Higashimori et al. [7] have designed and developed the tracing type jumping robot by utilizing a rotational type motor developed for a high-speed multifingered hand system [9]. They considered the influences of the ratio of the motor output to the mass and the leg length for the jump height. In this work, we discuss the jumping pattern generation for a serial link robot, as shown in Fig.1. By applying a genetic algorithm (GA) for torque assignment, we find the jumping pattern for achieving the maximum jump height under a torque limitation. Morimoto et al. [8] have discussed the stand up motion of a serial link robot by using reinforcement learning. These works focus on the reinforcement learning technique for the given specification of the robot. On the other hand, we especially focus on what jumping pattern can be found and what torque pattern is generated for achieving the maximum jump height under the given torque limitation and the joint angle limitation. In addition, we are interested in how the jumping pattern and the torque pattern change especially with the change in torque limitation.

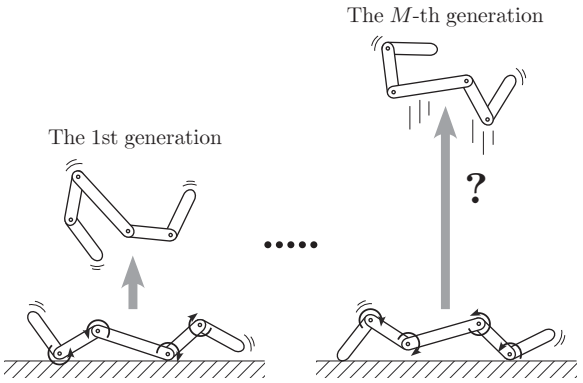

Fig. 1. The maximum jump height?

This paper is organized as follows: In section 2, we give the model for the serial link robot and define the problem formulation where we find the torque pattern leading the maximum jump height. We explain the way for generating the joint torque with respect to time, based on a GA and the dynamic simulation. In section 3, we evaluate the obtained jump heights of the serial link robot. By using the non-dimensional parameters composed of the joint torque, the leg length, and the mass, we show the transition of the effective jumping patterns for achieving the maximum jump height under the given mass of the robot and the torque limitation. When the joint torque is small compared with $w \cdot l$ where w and l are the weight and the length of the robot, it is difficult for the robot to jump. In this case, the robot lifts its center of the mass by both ends of the links and the robot can only jump a little bit. With the increase of the torque limitation, the robot obtains the capability to stand up with a single leg, and

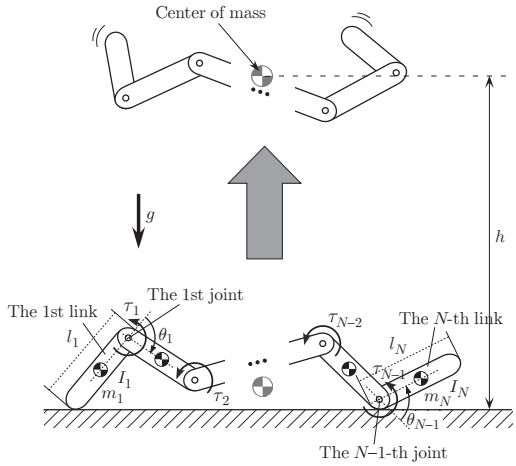

Fig. 2. Model for a serial link

finally jumps into the air. We show the spring-type jump where the robot has the initial posture folding over all links and it finally extend all links simultaneously. We further consider the jumping pattern under the joint angle limitation. We show an interesting jumping pattern where one end of the link is first lifted up and the other end finally kicks the ground strongly.

II. Procedure for Obtaining Jumping Patterns

A. Model for the Serial Link Robot

Suppose a serial N-link robot as shown in Fig.2, where l_i, m_i, $I_i (i = 1, \ldots, N)$, θ_j, $\tau_j (j = 1, \ldots, N-1)$, g, and h are the length of the i-th link, the mass of the i-th link, the moment of inertia of the i-th link, the angle of the j-th joint, torque of the j-th joint, the gravitational acceleration, and the maximum height of the center of the mass during a jumping motion, respectively. The body of the motor driving the j-th joint is fixed on the j-th link and the rotational axis of that is fixed to the $j+1$-th link, respectively. For the simplification, we assume that the mass of the motor is included in the mass of the link and the center of the mass of each link is located at the center of the link. We also give the joint angle limitation as $\theta_j^{\min} \leq \theta_j \leq \theta_j^{\max}$. While a regular DC servo motor has a decreasing characteristics with respect to angular velocity, there are a couple of AC servo motors producing an arbitrary torque by supplying current depending upon the angular velocity. In this work, we also suppose that the motor has the limitation by a maximum angular velocity of $\omega_{\max}$.

B. Problem Formulation for Finding the Optimum Jumping Pattern

The question is which jumping strategy to use in order to reach the maximum jump height by the serial link robot as shown in Fig.2. In this work, we focus on the joint torque pattern with respect to time and define the optimization problem as follows:

$$\begin{array}{ll} \text{Maximize} & F = h_{\max}(\tau_j(t)) \\ \text{Subject to} & \tau_j^{\min} \leq \tau_j(t) \leq \tau_j^{\max} \quad (j = 1, \ldots, N-1) \\ & 0 \leq t \leq T \end{array}$$

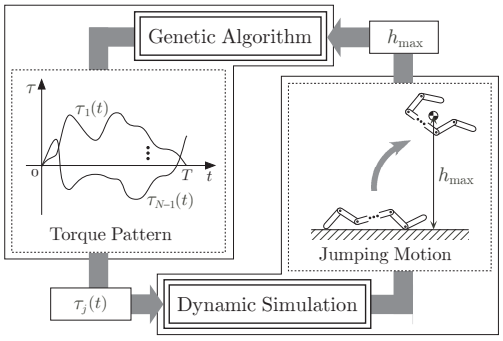

Fig. 3. Procedure for obtaining the maximum jumping pattern

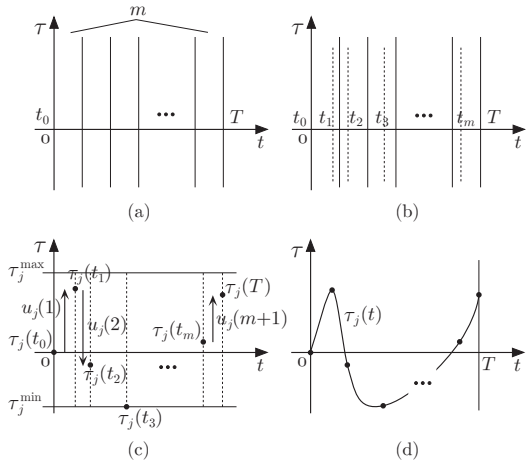

Fig. 4. Generation of joint torque with respect to time

where $\tau_j(t)$, $\tau_j^{\min}$, $\tau_j^{\max}$, and T are the function expressing the j-th joint torque with respect to time, the minimum and maximum torque limitation for the j-th joint, and the time for continuously controlling the robot, respectively. $h_{\max}$ is the maximum height of the center of the mass during all tested jumping motions.

C. How to obtain the jumping pattern

We utilize a GA to obtain the maximum jump height. As shown in Fig.3, we generate the jumping motion for each chromosome of $\tau_j(t)$ by a dynamic simulation and used $h_{\max}$ as the evaluation function.

Generation of joint torque with respect to time: Fig.4 shows how to generate the joint torque with respect to time. $\tau_j(t)$ under the torque limitation $\tau_j^{\min} \leq \tau_j \leq \tau_j^{\max}$ is generated by the following way:

(1) T is divided by m as shown in Fig.4(a), and $t_k (k = 0, \ldots, m+1)$ is set within each section as shown in Fig.4(b), where $t_0 = 0$, $t_{m+1} = T$.

(2) The joint torque at t_k is given by $\tau_j(t_k) = \tau_j(t_{k-1}) + u_j(k)$ as shown in Fig.4(c), where $u_j(k)$ is the uniform random number under $|u_j(k)| \leq \left|\tau_j^{\max} - \tau_j^{\min}\right|$ and $\tau_j(0)$ is given by zero, respectively. We change $\tau_j(t_k)$ to $\tau_j(t_k) = \tau_j^{\min}$ and $\tau_j(t_k) = \tau_j^{\max}$ in the case where $\tau_j(t) < \tau_j^{\min}$ and $\tau_j^{\max} < \tau_j(t)$, respectively.

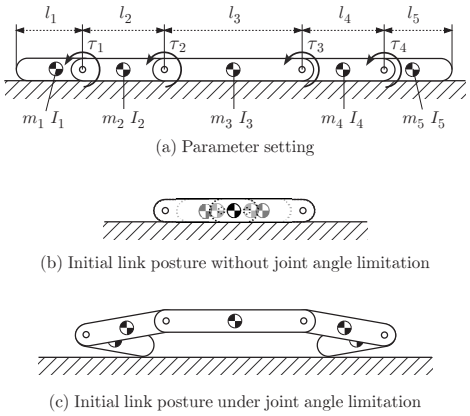

(a) Parameter setting

(b) Initial link posture without joint angle limitation

(c) Initial link posture under joint angle limitation

Fig. 5. Simulation model

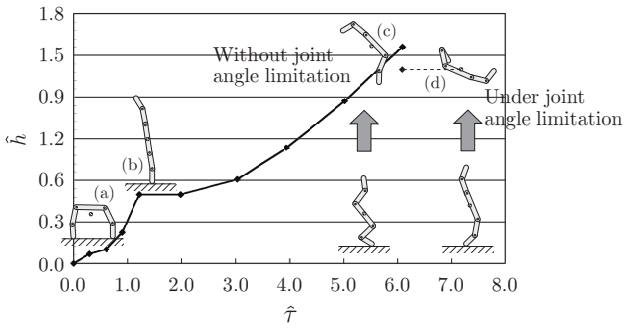

Fig. 6. Relationship between $\hat{\tau}$ and $\hat{h}$

(3) The function $\tau_j(t)$, which expresses the joint torque with respect to time, is generated by connecting $\tau(t_k)$ and $\tau(t_{k+1})$ step by step with a spline function as shown in Fig.4(d). We change $\tau_j(t)$ to $\tau_j(t) = \tau_j^{\min}$ and $\tau_j(t) = \tau_j^{\max}$ in the case where $\tau_j(t) < \tau_j^{\min}$ and $\tau_j^{\max} < \tau_j(t)$ are generated, respectively.

Since $\tau_j(t)$ is sensitive to both $u_j(k)$ and t_k, we utilize $u_j(k)$ and t_k as the parameters for finding the optimum $\tau_j(t)$.

Dynamic simulation: The simulation software ADAMS (MSC. Software, Corp.) is utilized for computing a dynamic motion of the robot with a given joint torque set with respect to time. By giving constraint and boundary conditions among objects, this software including mathematical models can execute dynamic simulations. We use the contact model where the virtual spring and dumping are assumed for each contact between two objects.

III. Transition of Jumping Pattern

A. Evaluation of Jump Height by Using Non-dimensional Parameters

To evaluate the maximum jump height $h_{\max}$ with consideration of the relative relationship between the scale (m_i, l_i) and the joint torque limitation $\left(\tau_j^{\min}, \tau_j^{\max}\right)$ of the robot, we introduce two non-dimensional parameters as follows:

$$\hat{h} = \frac{h_{\max}}{\sum_{i=1}^{N} l_i} \quad (1)$$

$$\hat{\tau} = \frac{\sum_{j=1}^{N-1} \max\{|\tau_j^{\min}|, |\tau_j^{\max}|\}}{\sum_{i=1}^{N} m_i g l_i} \quad (2)$$

$\hat{h}$ expresses the ratio of the maximum jump height to the total length of the robot, and $\hat{\tau}$ expresses the total torque, which can be instantaneously generated, normalized by the total of the maximum gravitational torque applied to each joint. Now, we consider the serial link robot with five links and four joints $(N = 5)$ as shown in Fig.5(a). The non-dimensional parameter $\hat{\tau}$ varies only by the change of $\tau_j^{\min}$ and $\tau_j^{\max}$, where $\tau_1^{\min} = \tau_2^{\min} = \tau_3^{\min} = \tau_4^{\min}$ and $\tau_1^{\max} = \tau_2^{\max} = \tau_3^{\max} = \tau_4^{\max}$. Other parameters are given as follows; $l_1 = l_5 = 60[\mathrm{mm}]$, $l_2 = l_4 = 75[\mathrm{mm}]$, $l_3 = 123[\mathrm{mm}]$, $m_1 = m_5 = 25[\mathrm{g}]$, $m_2 = m_4 = 75[\mathrm{g}]$, $m_3 = 140[\mathrm{g}]$, $I_1 = I_5 = 9.8[\mathrm{kgmm^2}]$, $I_2 = I_4 = 54[\mathrm{kgmm^2}]$, $I_3 = 230[\mathrm{kgmm^2}]$, $\omega_{\max} = 31.4[\mathrm{rad/s}]$, $T = 2.0[\mathrm{s}]$, and $m = 200$, respectively. In addition, the viscosity of the joint is given by $d_j = 53.0[\mathrm{Nmm \cdot s}](j = 1, \ldots, 4)$, and the virtual spring, the dumping, and the coefficient of friction for contacts between the link and the ground are given by $k = 1000[\mathrm{N/mm}]$, $d = 1.1[\mathrm{Ns/mm}]$, and $\mu = 0.58$, respectively.

Fig.6 shows the relationship between $\hat{\tau}$ and $\hat{h}$. Actually, $\hat{h}$ is obtained by the learning process as shown in section 2. The link postures in Fig.6 show the postures at the moment of taking off and those at the maximum point, where Fig.6(a), (b), and (c) are obtained for $\hat{\tau} = 0.91$, $\hat{\tau} = 1.22$, and $\hat{\tau} = 6.10$, respectively, under $-\infty \leq \theta_j \leq \infty$. In Fig.6(d), we also denote $\hat{h}$ and the link postures for $\hat{\tau} = 6.10$ under $\theta_j^{\min} = -160[\mathrm{deg}](j = 1, 4)$, $\theta_j^{\max} = 160[\mathrm{deg}](j = 1, 4)$, $\theta_j^{\min} = -90[\mathrm{deg}](j = 2, 3)$, and $\theta_j^{\max} = 90[\mathrm{deg}](j = 2, 3)$. Through preliminary simulations, we found that $\hat{\tau}$ is not much influenced by the initial link posture. We finally set up the initial link postures as shown in Fig.5(b) and (c) for the joint angle limitation in Fig.6(a)–(c) and (d), respectively. From Fig.6, we can see that $\hat{h}$ increases almost proportional to $\hat{\tau}$. The increase of $\hat{\tau}$ is equivalent to the increase of the joint torque or the decrease of the mass of the robot, and we can intuitively understand that such changes contribute to increase of $\hat{h}$ directly.

B. Double-leg Jump and Single-leg Jump around $\hat{\tau} = 1$

Fig.7 shows the result after the learning process where $\hat{\tau} = 0.91$ ($\tau_j^{\min} = -300[\mathrm{Nmm}]$, $\tau_j^{\max} = 300[\mathrm{Nmm}]$). Fig.8 shows the jumping pattern corresponding the best solution of the 50th generation. As shown in Fig.8, we can see that it is substantially difficult for the robot to jump because the joint torque is not large enough for lifting up the robot from the ground. The robot can jump only for a short time. In this case, the robot tries to lift up its center of the mass, where the pair of the 1st and the 2nd links and that of the 4th and 5th links are regarded as the left and the right leg, respectively.

On the other hand, Fig.9 shows the result after the learning process where $\hat{\tau} = 1.22$ ($\tau_j^{\min} = -400[\mathrm{Nmm}]$, $\tau_j^{\max} = 400[\mathrm{Nmm}]$). Fig.10 shows the jumping pattern generated by the best solution of the 50th generation. As shown in Fig.10, we can also see that it is actually difficult for the robot to jump for torque limits below $\hat{\tau} = 1.22$. In this case, however,

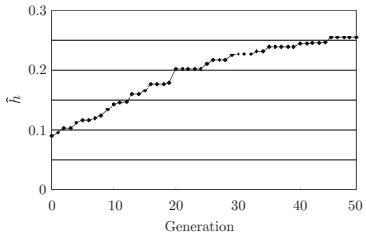

Fig. 7. Relationship between generation and $\hat{h}$ where $\hat{\tau} = 0.91$

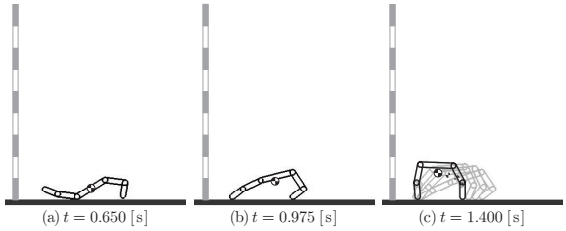

Fig. 8. Change of link posture with respect to time where $\hat{\tau} = 0.91$

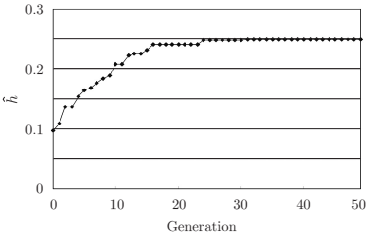

Fig. 9. Relationship between generation and $\hat{h}$ where $\hat{\tau} = 1.22$

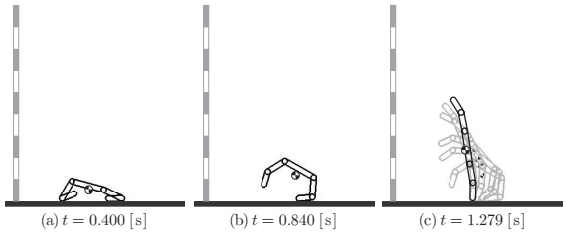

Fig. 10. Change of link posture with respect to time where $\hat{\tau} = 1.22$

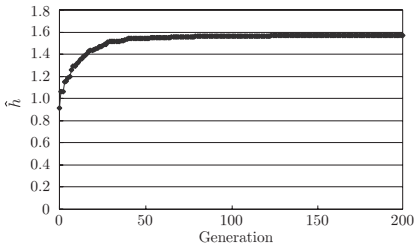

Fig. 11. Relationship between generation and $\hat{h}$ where $\hat{\tau} = 6.10$

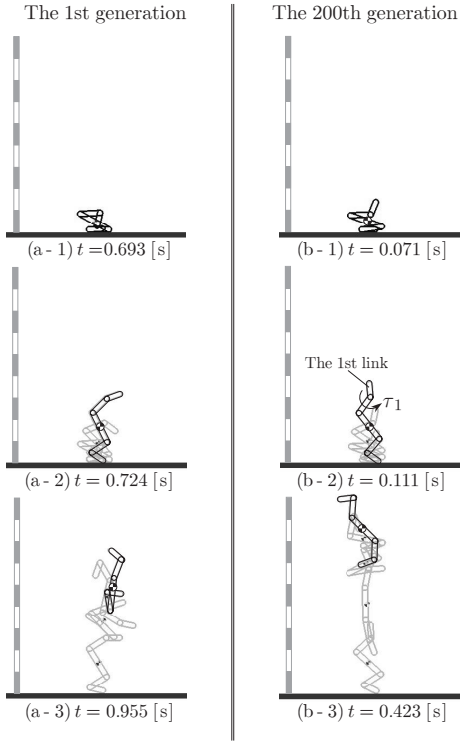

Fig. 12. Jumping pattern where $\hat{\tau} = 6.10$

the robot is able to lift the center of the mass by using single leg. We can see that the robot tries to establish a straight line with its link posture, so that it can lift the center of mass as high as possible.

From the above discussion, we would note that $\hat{\tau} = 1$ may be the index whether the robot can stand up by a single leg or not for a given mass. As a result, $\hat{\tau} = 1$ seems to provide us with the boundary at which the jumping pattern changes. However, it is difficult to achieve a practical jump with a parameter setting around $\hat{\tau} = 1$.

C. Spring-type jump under $\hat{\tau} > 1$

With the increase of $\hat{\tau}$, the robot can take off the ground and jump. But, what jumping pattern is effective to achieve the largest jump height? With the map shown in Fig.6, we can confirm that the jumping pattern to achieve the maximum jump height under $\hat{\tau} > 1$ converges to a single pattern. In this section, we consider the jumping pattern and the joint torque with respect to time where $\hat{\tau} = 6.10$.

Jumping pattern: Fig.11 shows the result after the learning process where $\hat{\tau} = 6.10$ ($\tau_j^{\min} = -2000$[Nmm], $\tau_j^{\max} = 2000$[Nmm]). Fig.12(a)–(b) show the jumping patterns leading to the best solutions after the 1st and the 200th generation, respectively. In the best solution after both generations, we can see that the robot obtains the upward motion by kicking the ground by folding the all links extremely as shown in Fig.12(a-1)–(a-2) and Fig.12(b-1)–(b-2). This behavior is just like the motion of spring after releasing. Especially, such a spring-like motion becomes more remarkable in the best solution after the 200th generation as shown in Fig.12(b-1)–(b-3). In such a jumping pattern, the work done by the joint actuators is effectively transformed into the upward translational kinetic energy by alternating the rotational direction between actuators, while rotational and horizontal translational energy of whole link system are hardly generated.

Joint torque with respect to time: Fig.13 shows the torque

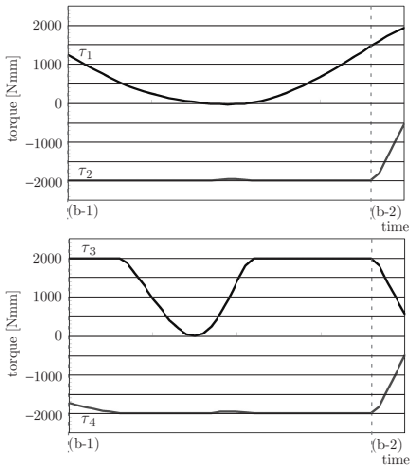

Fig. 13. Torque pattern of the 200th generation with respect to time where $\hat{\tau} = 6.10$

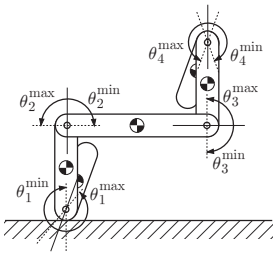

Fig. 14. Joint angle limitation

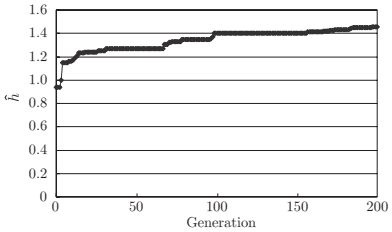

Fig. 15. Relationship between generation and $\hat{h}$ where $\hat{\tau} = 6.10$, under joint angle limitation

pattern for achieving the jumping pattern leading to the best solution of the 200th generation under $\hat{\tau} = 6.10$. Fig.13 (b-1) and (b-2) correspond to the time of Fig.12 (b-1) and (b-2), respectively. As shown in Fig.13, each joint torque is generated by switching the rotational direction so that the whole link behaves as if it is a spring. However, the maximum or minimum torque limit is not always given to each joint, and the joint torque is controlled so that the robot may take off perpendicular to the ground.

D. Jumping Pattern under Joint Angle Limitation

In the case where collisions between links are ignored, the robot can achieve a large jump height where it stretches out in the upward direction like a spring with the posture folding all links extremely at the initial phase. Now, let us consider the jumping pattern under the joint angle limitation as shown in Fig.14. Under such an angle limitation where the robot cannot fold each link completely, what jumping pattern is effective to achieve the largest jump height? In this section, we discuss the jumping pattern under the joint angle limitations given by $\theta_j^{\min} = -160[\deg](j = 1, 4)$, $\theta_j^{\max} = 160[\deg](j = 1, 4)$, $\theta_j^{\min} = -90[\deg](j = 2, 3)$, and $\theta_j^{\max} = 90[\deg](j = 2, 3)$.

Jumping pattern: Fig.15 shows the result after learning process under $\hat{\tau} = 6.10$ ($\tau_j^{\min} = -2000$[Nmm], $\tau_j^{\max} = 2000$[Nmm]). Comparing Fig.11 and Fig.15, the robot under the joint angle limitation has achieved as 92% high as the robot without the joint angle limitation. Fig.16(a) and (b) shows the jumping patterns leading to the best solution of the 1st and the 200th generation, respectively, under $\hat{\tau} = 6.10$. The best solutions of both the 1st and the 200th generation show the following same interesting features: First, the robot moves the center of the mass over the one end of leg, and the other end kicks the ground for generating the upward motion at the initial phase (Fig.16(a-3)–(a-4), Fig.16(b-3)–(b-4)). At the next phase, the robot kicks the ground with the support leg so that it can generate a big upward motion of the center of the mass. We can see that the motion where the robot shifts the center of the mass on the kicking leg and the motion where the robot expands links toward the take off, more remarkably and more smoothly in the best solution of the 200th generation. If the center of the mass is away from the line connecting the tip of the support leg and the center of mass, a large rotational energy and a horizontal translational energy are generated by the robot. On the other hand, the direction of reaction force coincides with that of the line connecting between the contact point at the support leg and the center of mass, we can expect that the work done by joint torque is efficiently transmitted into the translational kinetic energy in the vertical direction.

Joint torque with respect to time: Fig.17 shows the torque pattern for the jumping pattern leading to the best solution of the 200th generation where $\hat{\tau} = 6.10$. Fig.17 (b-1)–(b-5) corresponding to the time of Fig.16(b-1)–(b-5). As shown in the time history of joint torque Fig.17(b-1)–(b-3), both τ_3 and τ_4 are generated so that the 4th and the 5th links are folded to the inner direction, both τ_1 and τ_2 are generated so that whole the robot rotates in the clockwise direction by small kicking motion on the ground at the end of the 1st link. As a result, both the 1st and the 2nd links are lifted up and the center of the mass of the robot is moved onto the end of the 5th link. In the motion where the robot kicks the ground strongly as shown in Fig.17(b-3)–(b-5), both τ_3 and τ_4 driving the kick leg are generated with the full torque under the torque limitation. On the other hand, both τ_1 and τ_2 driving the free leg are generated strongly at the beginning, while they are decreased towards a take off. This is for controlling the links so that they finally make a straight line perpendicular to the ground. We would note that each joint is not always given the maximum or the minimum torque, but given the suitable torque for controlling the links so that the robot can move the center of the mass and kick the ground continuously and smoothly.

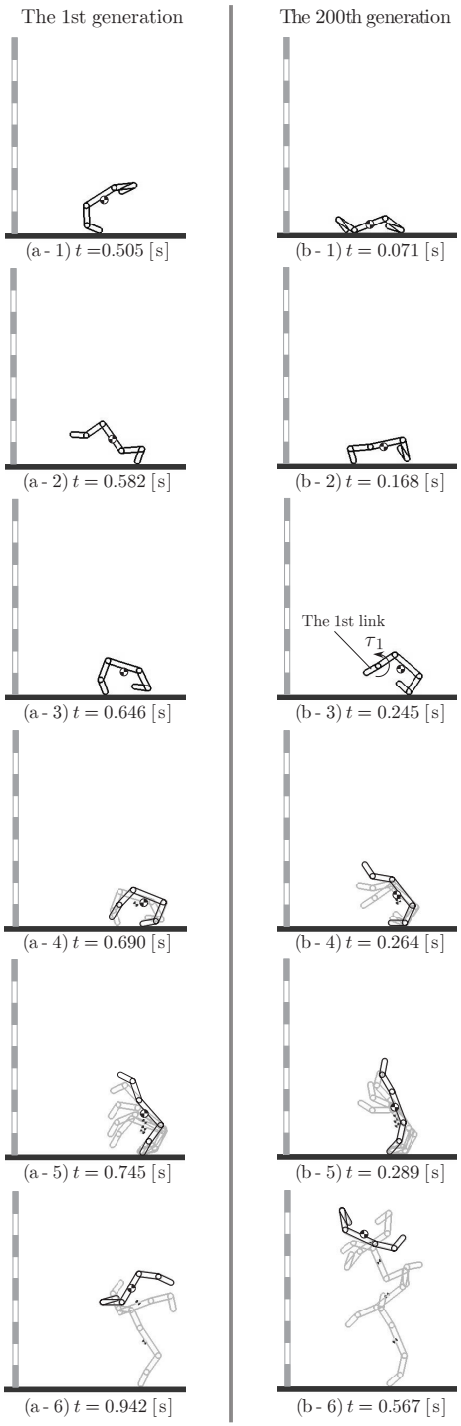

Fig. 16. Jumping pattern where $\hat{\tau} = 6.10$ under joint angle limitation

IV. Concluding Remarks

We discussed the jumping patterns for a serial link robot. The main results are summarized as follows:

(1) We evaluated the jump height with two non-dimensional parameters, by focusing on the relative relationship between the scale and the joint torque of the robot.

(2) With the increase of the torque limitation, the double-leg based jump, the single-leg based jump, and the spring-type jump were generated.

(3) Under the joint angle limitation, we also obtained an interesting solution where one end of the link is first lifted up and the other end finally kicks the ground strongly.

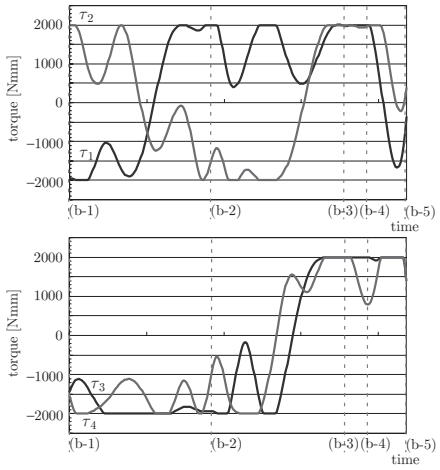

Fig. 17. Torque pattern of the 200th generation with respect to time where $\hat{\tau} = 6.10$, under joint angle limitation

The jumping patterns obtained in this paper may remind us of the jumps by human and animals. We expect that the jumping pattern of robot will become more similar to those of human and animals by matching their mechanisms, configurations, torque limitations, and angle limitations. We also would like to note that the method we introduced in this paper is not limited for the serial link mechanism but can be applied to parallel link mechanism.

References

[1] E. Nakano and H. Okubo, "Jumping Machines," Journal of the Robotics Society of Japan, vol.11, no.3, pp.342–347, 1993 (In Japanese).

[2] M. H. Raibert, H. B. Brown, Jr, and M. Chepponis: "Experiments in Balance with a 3D One-Legged Hopping Machine," The Int. Journal of Robotics Research, vol.3, no.2, pp.75–92, 1984.

[3] H. Okubo, M. Handa, and E. Nakano, "Design of a Jumping Machine using Self-energizing Spring – Jumping by Small Actuators –," Journal of the Robotics Society of Japan, vol.16, no.5, pp.633–639, 1998 (In Japanese).

[4] H. Tsukagoshi, Y. Mori, M. Sasaki, T. Tanaka, and A. Kitagawa: "Development of Jumping & Rolling Inspector to Improve the Debris Traverse Ability," Journal of Robotics and Mechatronics, vol.15, no.5, pp.482–490, 2003.

[5] R. Hayashi and S. Tsujio, "A Pendulum-type Jumping Machine Utilizing Human's Swing," Journal of the Robotics Society of Japan, vol.19, no.4, pp.528–534, 2001.

[6] K. Arikawa and T. Mita: "Design of Multi-DOF Jumping Robot," IEEE Proc. of Int. Conf. on Robotics and Automation, pp.3992–3997, 2002.

[7] M. Higashimori, M. Harada, M. Yuya, I. Ishii, and M. Kaneko: "Dimensional Analysis Based Design on Tracing Type Legged Robots," Proc. of the IEEE Int. Conf. on Robotics and Automation, pp.3744–3749, 2005.

[8] J. Morimoto and K, Doya: "Acquisition of Stand-up Behavior by a Real Robot using Hierarchical Reinforcement Learning," Proceedings of International Conference on Machine Learning, pp.623–630, 2000.

[9] A. Namiki, Y. Imai, M. Ishikawa, and M. Kaneko: "Development of a High-speed Multifingered Hand System and Its Application to Catching," In Proc. of IEEE/RSJ Int. Conf. on Intelligent Robots and Systems, pp.2666–2669, 2003.